

COMPARISON OF CARBON-BONDED ALUMINA FILTERS WITH ADDITION OF TITANIA AND NANOMATERIALS IN CONTACT WITH A STEEL MELT

Enrico Storti¹, Steffen Dudczig¹, Gert Schmidt¹, Christos G. Aneziris¹

¹TU Bergakademie Freiberg, Freiberg, Germany

ABSTRACT

In order to improve the filtration efficiency of ceramic filters, carbon-bonded alumina filters were coated with multi-walled carbon nanotubes and alumina nanosheets. The samples were tested for different times in contact with a steel melt containing endogenous inclusions at 1650°C. Investigation of the filters after the test was carried out by optical and scanning electron microscopy. In addition, steel samples were analyzed with a special automatic SEM. The population of detected inclusions was classified in terms of size and chemistry.

Keywords: Ceramic foam filters, Carbon nanotubes, Alumina nanosheets, Non-metallic inclusions

INTRODUCTION

Non-metallic inclusions in cast metal parts usually have a detrimental effect on the properties of the components. They can cause internal cracks, slivers, or blisters in final rolled products. Moreover, large macro-inclusions as well as inclusion clusters severely degrade the mechanical properties^[1]. In 2008, due to axle fracture an ICE 3 high-speed train derailed after leaving the Cologne train station in Germany. The fracture was associated to large agglomerated alumina particles, which were probably formed during the casting process from smaller endogenous inclusions^[2]. Therefore, especially for safety relevant components, it is crucial to improve the cleanliness of the metal melts: high purity can be achieved by using a filtration process after the ladle treatment^[3]. In the case of steel, ceramic foam filters (CFFs), especially those based on zirconia and carbon-bonded alumina, have been successfully employed for years.

As recently reported by Dudczig et al., carbon-bonded alumina filters react when immersed in a steel melt and produce a new thin, dense alumina layer (identified as crystalline α -alumina at room temperature) on the contact area with the steel^[4]. In order to explain this phenomenon, a postulated mechanism involves the reduction of the primary alumina grains of the filter by the carbon, with formation of aluminum suboxides: these then react with the oxygen dissolved in the melt and produce the secondary alumina^[5]. Thermodynamic studies have suggested a different mechanism, which involves a partial dissolution of alumina and carbon into the liquid metal at the interface. Afterwards, this liquid reacts with some fresh steel promoting the precipitation of the secondary alumina layer^[6]. Thanks to the new metal/alumina interface, the steel melt suddenly exhibits a poor wettability toward the filter while the chemistry and crystallographic structure of the surface are changed to that of the inclusions. As a consequence the newly formed layer can efficiently remove these impurities from the melt. The material buildup on a carbon-bonded alumina filter after a 60 s immersion test, as discussed by Dudczig et al., generally presents the following structures (from the center of a strut to the surface)^[4]:

- A. Unaffected carbon-bonded substrate
- B. Decarbonized layer of partially sintered alumina
- C. Oxide functional coating - from the production process (optional)
- D. Secondary, thin alumina layer - from the in situ reaction

- E. Dense collection zone mainly consisting of sintered, polyhedral endogenous alumina inclusions
- F. "Coral-like" zone consisting of endogenous alumina particles in complex shapes.

For good filtration results, a fast formation of the D layer is beneficial. Storti et al. have recently applied a MWCNTs-based coating on carbon-bonded alumina filters, in order to accelerate the formation of the thin alumina layer and to possibly improve the filtration efficiency^[7]. These filters were tested together with uncoated Al_2O_3 -C samples in a so-called metal casting simulator: 10 ppi (pores per inch) prismatic foam samples ($125 \times 20 \times 20 \text{ mm}^3$) were immersed into molten steel at 1650°C, containing artificially-generated endogenous alumina inclusions, under a fully controlled Ar atmosphere. Microscope investigations after the test suggested a better performance of the MWCNTs-coated filters compared to the uncoated ones, at least for short immersion times (10/30 s)^[8]. However, depending on the casting weight ceramic filters could be also employed for longer times, so new tests are required. In addition, the effect of the varying filter functionalization on the steel cleanliness is also of major importance. Based on the previous results, alumina nanosheets were added to the MWCNTs-based coating and new immersion tests were carried out. The inclusions remaining in the steel were thoroughly analyzed and classified by size and chemistry by means of a special scanning electron microscope.

MATERIALS AND METHODS

Filter production

The raw materials used for the preparation of the Al_2O_3 -C filters were aluminum oxide (Martinswerk, Germany, 99.80 wt.% $\text{Al}_2\text{O}_3 \leq 3.0 \mu\text{m}$), modified coal tar pitch powder (Rütgers, Germany, $d_{90} < 0.2 \text{ mm}$ – used as a binder as well as a carbon source), fine natural graphite (Graphit Kropfmühl, Germany, 96.7 wt.% carbon, 99.8 wt.% $< 40 \mu\text{m}$), and carbon black powder (Lehmann & Voss & Co., Germany, carbon content $\leq 99.0 \text{ wt.}\%$, ash content $> 0.01 \text{ wt.}\%$, primary particle size of 200-500 nm). The additives were ligninsulfonate (Otto-Dille, Germany – used as wetting agent and temporary binder), modified polycarboxylate ether (BASF, Germany – used as a dispersing agent), and alkylpolyalkyleneglycolether (Zschimmer & Schwarz, Germany – used as an antifoam agent). The carbon-bonded filters (10 pores per inch, $125 \times 22 \times 22 \text{ mm}^3$) were produced via the Schwartzwalder process using a two-steps approach, according to the parameters described by Emmel et al.^[9]. After drying, the filters were heat treated in retorts filled with calcined petcoke (Müco, Germany) with a particle size between 0.2 and 2 mm, to approach reducing conditions. The maximum temperature of 800°C was reached with a heating rate of 1 K/min, additional dwell steps of 30 min for every 100°C, and a final holding time of 180 min at 800°C. The raw materials used for the preparation of the coatings were MWCNTs (Chengdu Organic Chemicals, Chengdu, China, purity $> 95\%$, outer diameter $> 50 \text{ nm}$, length = 10-20 μm), Al_2O_3 -nanosheets (Sawyer, Eastlake, USA, α - Al_2O_3 , purity $> 97\%$, thickness 10-35 nm, width 0.5-3.0 μm) and modified coal tar pitch powder (see above – used as a binder). The additives were Xanthan powder (Erbslöh, Krefel, Germany –

used both as a dispersing agent and thickening agent), carboxylic acid preparation (Zschimmer & Schwarz, Germany – used as dispersing agent) ammonium-ligninsulfonate and alkylpolyalkyleneglycolether. The carbon nanotubes and Al_2O_3 –nanosheets (abbreviated as ANSs) were not purified before use. The preparation and application of the nano-coating on carbon-bonded alumina filters was performed as follows. Xanthan was first coupled with pulsed ultrasonication to disperse the nanotubes in water^[7]. The alumina nanosheets were dispersed separately in water in the same way, stabilized with Xanthan and then mixed with the CNTs dispersion in a 3:1 ratio (CNTs:ANSs). Finally, the coal tar pitch powder was added from another dispersion prepared by horizontal ball milling. After application and drying of the coating, the filters were thermally treated again under reducing conditions (see above) in order to achieve the bonding of the nanosized materials and close some residual porosity and cracks.

Melting experiment

A metal casting simulator (Systec, Germany) located at the Institute of Ceramic, Glass and Construction Materials in Freiberg was used to evaluate the purification behavior of nano-coated Al_2O_3 -C filters at different immersion times. Before melting, the casting simulator was evacuated to a pressure of 2 mbar and filled with Ar 4.6 (purity = 99.996 %). The whole procedure was performed twice. Next, ≈ 40 kg of commercially available 42CrMo4 steel (AISI 4142) were melted in a special crucible: this consisted of hydratable alumina-bonded alumina/alumina-magnesia-spinel material, without any silica, calcia or further additions (to prevent unwanted reactions during the experiment), presintered at 1600°C for 2h. The oxygen content and the temperature of the steel melt were measured with a po_2/T -sensor system (Heraeus Electro-Nite, Germany) at different stages of each test. Before the immersion of the filter samples, defined alumina impurities were created in the steel melt according to the procedure described by Dudczig^[4]. Once the desired temperature was reached, 0.5 wt.% (related to the steel mass) of an iron oxide mixture were added. Accordingly, the dissolved oxygen rose from 20-30 ppm up to 60-70 ppm. At this point, endogenous alumina inclusions were generated by adding 0.05 wt.% (again related to the steel mass) of pure aluminum metal to the melt. Only about 10 ppm [O] were detected after this step. Finally, the ceramic foam samples were dipped into the melt (at a temperature of $\approx 1650^\circ\text{C}$) and rotated with 30 revolutions per minute for 10 and 60 s, respectively. One steel melt was only used as reference and thus no filter was immersed in this case. All “finger-tests” were carried out under fully controlled argon atmosphere. At the end all samples were removed from the melt and cooled down in a chamber under argon in order to prevent oxidation of the carbon fraction.

Inclusion analysis

After solidification, the cylindrical steel blocks were cut and prismatic samples with approximate dimensions of $5 \times 5 \times 2$ cm³ were sawed from a standard position (i.e. at 2/3 height, 1/3 diameter from the edge). These metallographic specimens were mounted, carefully grinded and polished down to 1 μm . Next, the samples were analyzed by means of a special, automatic SEM (FEI, USA): areas of approximately 110 mm² were scanned for about 8 h. Inclusions > 0.6 μm were detected using a BSE (back-scattered electron) detector based on contrast difference with the steel matrix. For each found particle the AFA (automatic feature analysis) included position, geometry, orientation and chemical composition, this last one being carried out by EDS (energy-dispersive X-ray spectroscopy).

Afterwards, the inclusions were classified by composition according to the rule-file presented in Table 1. Rule-files are not commonly available and must be developed using reference specimens of known composition. In the table, “Dirt” refers to spots with very high carbon content, which could indicate the presence of organic residuals on the sample. “Fe-scratch” relates to abrasions left by the preparation process. “Others” refers to any composition that did not match our rule-file. Iron oxide was likely formed by corrosion of the surface after removal of an inclusion during the polishing process.

Table 1: Rule file used for the automatic SEM analysis to classify the inclusions found in the solidified steel samples.

Chemical class	Element content [mol%]
Al_2O_3	$\text{Al} > 8$ and $\text{O} > 8$ and $\text{Mn} < 10$ and $\text{S} < 8$ and $\text{Ca} < 5$
Ca-aluminate	$\text{Ca} > 10$ and $\text{Al} > 5$
Mg-spinel	$\text{Al} > 8$ and $\text{Mg} > 0$ and $\text{S} < 5$ and $\text{Ca} < 5$
Al-Mn-Mg-Fe-Ca-silicate	$(\text{Si}/\text{Al}) > 0.4$ and $(\text{Al} + \text{Mn} + \text{Mg} + \text{Ca}) > 10$
SiO_2	$(\text{Si}/\text{O}) \geq 0.4$ and $(\text{Si}/\text{O}) < 6.2$ and $\text{Al} < 3$ and $\text{Mg} < 3$ and $\text{Ca} < 3$ and $\text{K} < 3$ and $\text{Mn} < 5$ and $\text{S} < 10$
MnO-MnS	$\text{Mn} > 8$ and $(\text{Mn}/\text{S}) > 2$ and $\text{Al} < 20$ and $\text{Si} < 5$ and $\text{Ca} < 5$
CaO-CaS	$\text{Ca} > 5$ and $(\text{Ca}/\text{S}) < 2$
Dirt	$\text{C} > 10$
Fe-oxide	$\text{Fe} > 60$ and $\text{O} > 20$ and $(\text{Si} + \text{Al} + \text{Mn} + \text{Mg} + \text{Ca} + \text{Na}) < 10$
Fe-scratch	$\text{Fe} > 90$
Other	True

RESULTS AND DISCUSSION

The carbon-bonded filters were able to withstand the strong thermal shock and high temperature conditions. According to our sensor, the dissolved oxygen only rose up to 20-30 ppm after the test (i.e. close to the initial value), regardless of the immersion time. The fluctuations were likely related to the slight temperature difference. No macroscopic damage was observed on the filters after the test and only the areas which were in direct contact with the melt showed a color change from black to gray: this was related to decarburization of the surface and formation of a new phase at the contact with the steel melt.

Table 2: Melt conditions after filter immersion.

Immersion time	Final temperature	Dissolved oxygen
10 s	1651 °C	21 ppm
60 s	1656 °C	27 ppm

Optical micrographs of the filters after the immersion tests are presented in Figures 1-2 (only the affected part is shown). As observed in previous studies^[8], with increasing time the surface also showed a rougher and brighter appearance. Very limited damage in the form of cracks was observed, which appeared to be partially sealed after 60 s thanks to the formation and

progressive growth of new layers on the surface. Moreover, some steel (mainly in the form of spherules) was collected on the surface or in the macropores.



Figure 1: Optical micrograph of the filter surface after 10 s of contact with the steel melt.

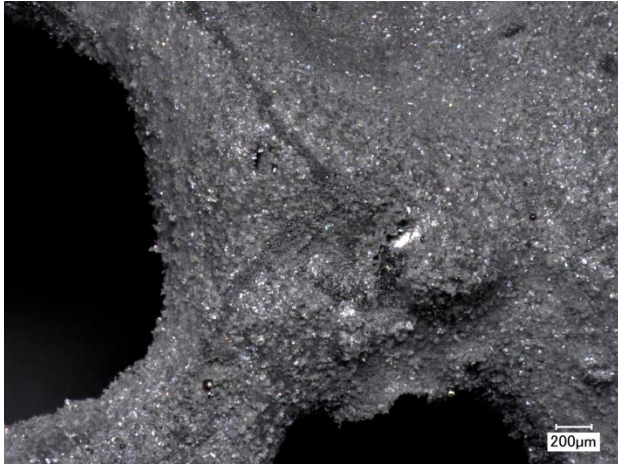


Figure 2: Optical micrograph of the filter surface after 60 s of contact with the steel melt.

SEM micrographs of the filter surface after contact with the steel melt are presented in Figures 3-5. Alumina inclusions with plate-like shape were found on all samples. However, after 10 s of interaction, the so-called layer F was still in the initial development. Where the sample was damaged either by handling or preparation, the typical layer buildup described in the Introduction was confirmed. After longer contact time, a thicker clogging layer consisting of sintered alumina particles was detected. In addition, many clusters of nano-sized inclusions with dendritic shape were found on top of this layer after 60 s. Similar particles were detected by Schmidt et al. on alumina-coated filters after the same contact time^[10]. We believe that these particles are the actual endogenous inclusions produced by our treatment before the immersion test. According to Dekkers, at very high oxygen and aluminum supersaturation, growth of alumina inclusions becomes unstable and the crystal corners grow along the supersaturation gradient, which may result in the formation of dendrites^[11]. On the other hand, layers E and F mainly consist of plate-like particles that should derive from the reaction of the filter material at the interface with the molten steel, as described by Schmidt et al. ANSs were not observed on the tested samples and were likely

involved in the formation of the thin layer D or of the plate-like particles. CNTs were quickly dissolved thanks to their high specific surface area.

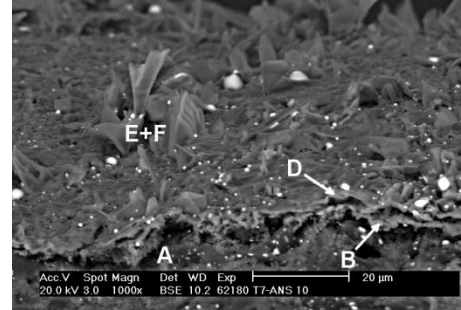


Figure 3: Overview of the surface after 10 s immersion test.

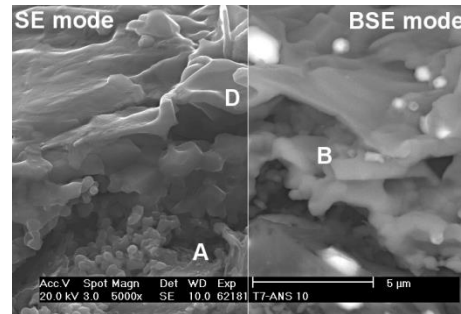


Figure 4: Detail of the layer buildup after 10 s immersion test.

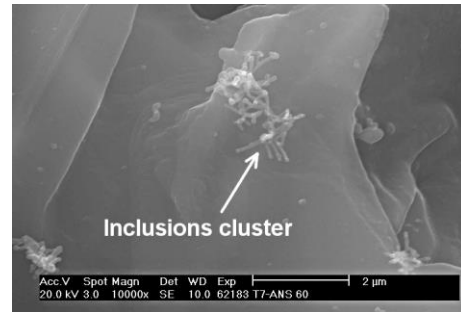


Figure 5: Cluster of fine inclusions found after 60 s test.

Table 3: Number of inclusions found in the steel samples by automatic SEM analysis, classified by chemistry. Values for alumina-coated filters reported by Schmidt et al.^[10]

Chemical class	Inclusions per cm ²				
	No filter	Al ₂ O ₃ -coated 10 s	CNTs-ANSs 10s	Al ₂ O ₃ -coated 60 s	CNTs-ANSs 60 s
Al ₂ O ₃	1248	371	56	439	446
Ca-aluminate	0	0	0	0	0
Mg- spinel	0	0	0	0	0
Al-Mn-Mg-Fe-Ca-silicate	0	0	2	0	234
SiO ₂	5	9	1	18	3
MnO-MnS	6	0	0	0	1
CaO-CaS	0	0	0	0	0
Other	116	9	1	16	81

The inclusions found by means of automatic SEM on the steel surfaces are presented in Table 3, classified by chemistry according to the rule file presented in Table 1. It has to be noted that these numbers represent the particles left in the solidified steel after testing the filters in the steel casting simulator, hence lower values would indicate a better purification efficiency, assuming our steel samples were significant. Since “Dirt”, “Fe-oxide” and “Fe-scratch” do not represent actual inclusions, they are not listed here. In addition, when analyzing the composition of “other” inclusions, almost only Fe and O were found. This means that the majority of such inclusions could be also classified as “Fe-oxide” or “Fe-scratch”, lowering the number of actual inclusions. In a recent contribution, similar filters with a pure alumina coating were tested in our same conditions^[10]. The results are also presented in Table 3 for comparison. The majority of inclusions in the reference melt (not filtered) consisted of Al₂O₃, as expected due to the oxide/Al treatment. In addition, silica was likely produced from the impurities in the raw materials. Calcium aluminate and magnesium spinel probably never developed during the immersion tests thanks to the low Ca and Mg available in the steel. Regarding the inclusion size, most of the detected particles in the steel samples had a surface area <20 µm², while only few inclusions were >50 µm². The presence of fine inclusions on the filter surface after the test would confirm this observation. It was generally observed that the use of a filter had a positive impact on the steel purity, especially for a 10 s immersion. Considering only Al₂O₃, the filtration efficiency of the nano-coated filters was approximately 95% for the 10 s test, versus 70% of the alumina-coated one. However, the 60 s experiments delivered only about 65% efficiency, with the nano-coated filter producing silicates in the steel as a side effect. This downside is consistent with the observations by Storti et al.^[12] Based on these results, we believe that our filters may be well suited for small castings. Depending on the steel quality, improving the filter capacity (available surface area) allows for shorter casting times. The efficiencies we obtained were quite impressive, considering that calculations predict a maximum filtration rate of only 24% and 18% for 10 and 30 ppi filters, respectively^[13]. It should be noted, though, that the model by Asad et al. does not yet consider the presence of gas bubbles in the melt or any chemical interaction between ceramic filter and inclusions. Moreover, within the model the prismatic filter is not rotating as in the real setup. The model will be improved in the future.

CONCLUSIONS

Carbon-bonded alumina filters were functionalized with a coating based on MWCNTs and alumina nanosheets. During the test in contact with molten steel at 1650 °C, the filters developed the typical layer structure previously reported by other authors. After 60 s of contact, fine endogenous inclusions (artificially generated before the test) were collected on the top layer. From the automatic SEM analysis on the steel samples after the test, fewer inclusions were found for the 10 s immersion, with a filtration efficiency of about 95%. For comparison, alumina-coated filters achieved 70% efficiency for the same contact time. On the other hand, the 60 s immersion only delivered a 65% filtration rate (for Al₂O₃) and produced new inclusions which were classified as mixed silicates.

ACKNOWLEDGEMENTS

The authors would like to thank Mrs. C. Ludewig and Mr. L. Lange for sample preparation, Dr. G. Schmidt for the SEM investigations, Mr. D. Thiele and Mr. R. Fricke for support during the test in the steel casting simulator. The studies were

carried out with financial support from the German Research Foundation (DFG) within the framework of the Collaborative Research Center SFB 920 “Multi-Functional Filter for Metal Melt Filtration – A Contribution towards Zero Defect Materials”.

REFERENCES

- [1] Zhang L. Nucleation, growth, transport, and entrapment of inclusions during steel casting. *Jom*. 2013; 65(9):1138–44.
- [2] Klinger C, Bettge D. Axle fracture of an ICE3 high speed train. *Eng Fail Anal*. 2013; 35(July 2008):66–81.
- [3] Apelian D, Mutharasan R, Ali S. Removal of inclusions from steel melts by filtration. *J Mater Sci*. 1985; 20:3501–14.
- [4] Dudczig S, Aneziris CG, Emmel M, Schmidt G, Hubalkova J, Berek H. Characterization of carbon-bonded alumina filters with active or reactive coatings in a steel casting simulator. *Ceram Int*. 2014; 40(10):16727–42.
- [5] Khanna R, Ikram-Ul Haq M, Wang Y, Seetharaman S, Sahajwalla V. Chemical Interactions of Alumina-Carbon Refractories with Molten Steel at 1823 K (1550 °C): Implications for Refractory Degradation and Steel Quality. *Metall Mater Trans B*. 2011; 42(4):677–84.
- [6] Zienert T, Dudczig S, Fabrichnaya O, Aneziris CG. Interface reactions between liquid iron and alumina-carbon refractory filter materials. *Ceram Int*. 2015; 41(2):2089–98.
- [7] Storti E, Emmel M, Dudczig S, Colombo P, Aneziris CG. Development of multi-walled carbon nanotubes-based coatings on carbon-bonded alumina filters for steel melt filtration. *J Eur Ceram Soc*. 2015; 35(5):1569–80.
- [8] Storti E, Dudczig S, Schmidt G, Colombo P, Aneziris CG. Short-time performance of MWCNTs-coated Al₂O₃-C filters in a steel melt. *J Eur Ceram Soc*. 2016; 36(3):857–66.
- [9] Emmel M, Aneziris CG. Development of novel carbon bonded filter compositions for steel melt filtration. *Ceram Int*. 2012; 38(6):5165–73.
- [10] Schmidt A, Salomon A, Dudczig S, Berek H, Rafaja D, Aneziris CG. Functionalized Carbon-Bonded Filters with an Open Porous Alumina Coating: Impact of Time on Interactions and Steel Cleanliness. *Adv Eng Mater*. 2017:1700170.
- [11] Dekkers R, Blanpain B, Wollants P. Crystal growth in liquid steel during secondary metallurgy. *Metall Mater Trans B*. 2003; 34:161–71.
- [12] Storti E, Dudczig S, Hubálková J, et al. Impact of nanoengineered surfaces of carbon-bonded alumina filters on steel cleanliness. *Adv Eng Mater*. 2017.
- [13] Asad A, Werzner E, Demuth C, et al. Numerical Modelling of flow conditions during steel filtration experiments. *Adv Eng Mater*. 2017.